ON TYRE BLOWOUTS AND OVERHEATING BRAKES TOWARDS SAFER TRUCKS

J. SUBEL
University of the Witwatersrand, Johannesburg

Obtained a BSc in 2017 from the University of the Witwatersrand. Currently undertaking an M.Sc. on heat transfer in heavy vehicle wheels.

F.W. KIENHÖFER
University of the Witwatersrand, Johannesburg

Associate Professor at the University of the Witwatersrand. Researching brake systems, PBS and developing lightweight automotive components.

J.H. LANGE
University of the Witwatersrand, Johannesburg

Obtained a BSc and an MSc from the University of the Witwatersrand in 2013 and 2015 respectively. Currently undertaking a PhD.

Abstract

Brake failure and tyre blowouts can have catastrophic consequences for heavy vehicles. Both events have been linked to excessive braking but the impact of wheel configuration on brake and tyre temperature is ill-understood. Dual and single wheels with steel and aluminium rims were tested on a custom-built rig at $1\ kW$ to $4\ kW$ alpine (or continuous) braking and the brake and tyre temperatures compared. Single wheels exhibited an average maximum tyre temperature increase 82% higher than the duals due to their lower convective surface area. The aluminium rims' higher thermal conductance caused an average maximum tyre temperature increase of 15% over the steel-rimmed wheels. Single wheels and aluminium rims increase the risk of tyre blowout due to overheating brakes, however configuration has no significant effect on brake temperature. Second-order, lumped-mass models for tyre and brake temperature are presented and evaluated. Maximum tyre temperature can be accurately predicted but brake temperature cannot be modelled using linear systems owing to radiative cooling effects.

Keywords: Aluminium Rims, Steel Rims, Single Wheels, Dual Wheels, Alpine Braking, Blowout, Tyre Failure, Brake Overheating, Lumped-Mass Modelling.

1. Introduction

Truck safety is of worldwide importance because unsafe trucks cause lives to be lost. In South Africa, 131 major truck accidents occurred between 2013 and 2016; resulting in 726 injuries and 791 casualties (RTMC, 2016). In 2016, the Road Traffic Management Corporation investigated 36 heavy vehicle collisions in which 136 people were injured and 143 killed (RTMC, 2017). Of the 131 accidents, vehicle-related factors were the second most common cause. This includes catastrophic brake and tyre failure. It follows that poor maintenance and unroadworthy vehicles exacerbate the frequency and severity of truck accidents.

Elevated temperatures accelerate the mechanical wear of the brakes and surrounding components. The surfaces of drum brakes have been measured at up to 900 ℃ which drastically increases wear, decreases braking performance and may lead to thermal cracking (Zhao *et al.*, 2008). At such high braking temperatures, proximate components are severely heated due to the dispersion of braking power; causing these components to experience dangerously high temperatures. For tyres, exposure to temperatures between $90\,℃ - 120\,℃$ results in a substantial decrease in fatigue life (Sokolov, 2009). Excessive brake temperatures have been linked to tyre fires by Hart (2012) and blowouts by Benoit *et al*. (2009).

Truck wheels are available in either dual or single configurations which are illustrated and compared in Figure 1. Rims for both configurations are manufactured from either steel or aluminium. Singles can offer up to 50% weight savings which translates into increased payload and improved fuel economy.

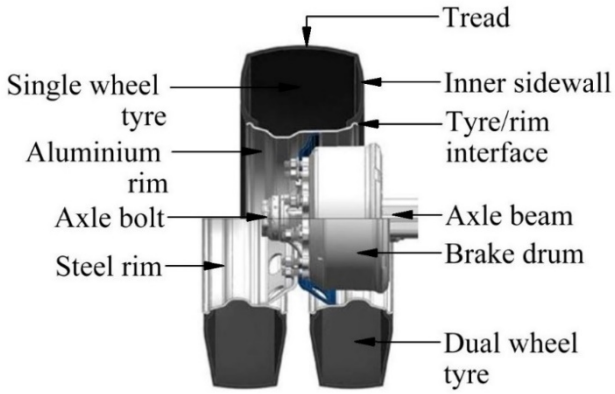

Figure 1 - Comparison of Dual and Single Wheel Configurations (Malzahn 2014)

Malzahn & Kienhöfer (2014) showed that single, aluminium-rimmed wheels have higher tyre temperatures for alpine braking profiles. Alpine braking is defined as the braking to keep a vehicle's speed constant when descending a slope i.e. an approximately constant braking power is continuously dissipated for prolonged periods of time. Brake dragging, which occurs when the friction surfaces do not fully disengage after the brakes are released, will also result in continuous braking.

Little work has been done to describe the propagation of braking heat throughout the wheel assembly. Consequently, designers are unable to reliably predict the risks of tyre overheating without performing finite element or finite difference analyses. There is a need for simplified models which can approximate the temperature response of wheel components to braking. First-order, lumped-mass models - as presented by Day (2014) - have proven effective in describing brake temperature in terms of bulk parameters, for example: mass, density, thermal conductivity and specific heat. The advantage of this method is that temperature response can be readily calculated with limited knowledge of the wheel's construction and geometry.

This paper compares the brake and tyre temperature responses of four wheel configurations to alpine braking across different braking powers. Generalised, second-order, lumped-mass models are presented and validated for brake shoe and maximum tyre temperature.

2. Objectives

- To measure and compare the brake and tyre temperatures of aluminium-rimmed and steel-rimmed wheels in dual and single configuration under $1\ kW$ to $4\ kW$ of continuous braking.
- To determine whether certain rim materials or wheel configurations are at an increased risk of tyre failure or brake overheating and identify the physical parameters which contribute to excessive component temperatures.

3. Research Approach

A custom-built rig (Figure 2) was used to emulate alpine braking. The rig consists of a BPW Eco Plus 2 axle fitted with drum brakes. Steel and aluminium rims were tested in both dual and single configurations. Further details of the rims and tyres are listed in Table 1. A vertical load of $20\ kN$ was applied to the axle to induce hysteresis heating. The wheel was run at $20\ km/h$ for four hours to reach thermal steady state. Thereafter the brakes were applied at constant braking powers (P_b) of $1\ kW$, $2\ kW$, $3\ kW$ and $4\ kW$. The brakes were applied for four hours to allow the temperatures to reach steady state.

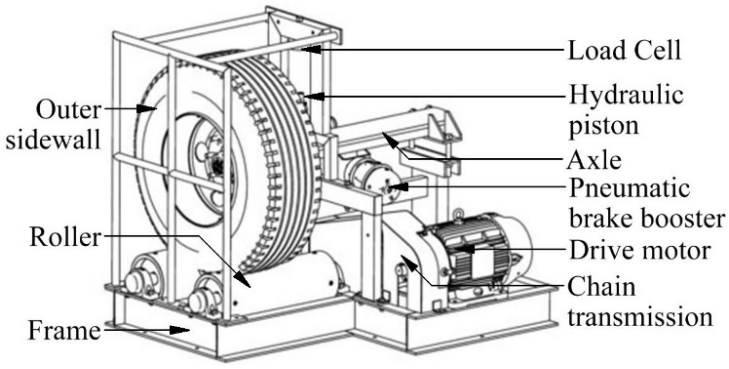

Figure 2 - University of the Witwatersrand Rolling Road

Table 1 – Summary of Wheel Configurations

Configuration	Rim			Tyre	
	Model	Mass, m $[kg]$	Thickness, t $[mm]$	Model	Mass, m $[kg]$
Dual, Steel	Unknown	32.5	12.0	$315/80\ R22.5$ Dunlop Transteel 811	67.0
Dual, Aluminium	Speedline SL830	28.0	24.5	$315/80\ R22.5$ Dunlop SP 391	70.5
Single, Steel	Unknown	53.5	13.0	$385/65\ R22.5$ Firestone TSP 3000 II	71.5
Single, Aluminium	Speedline SL291	26.0	26.0	$385/65\ R22.5$ Dunlop Transteel 833	75.5

Information on the exact compositions of the rims and tyres is not publically available. Thermophysical properties for steel, aluminium and automotive rubber (Table 2) were therefore assumed based on data available in literature (Welty, Rorrer and Foster, 2015, Luo *et al.*, 2015).

Table 2 - Approximate Material Properties

Material	Conductivity, k $[W/(m \cdot ℃)]$	Specific Heat, C_p $[J/(kg \cdot ℃)]$
Steel	60.5	434.0
Aluminium	229.0	938.3
Rubber	0.3	1800

A J-type thermocouple measured the temperature of the brake shoe while a FLIR T640 thermal imaging camera recorded the radial temperature distribution in the inner sidewall of the tyre. This region was chosen as it is the closest to the brake and is estimated to undergo the highest temperature change. The sidewall is also the most likely location for blowout to occur.

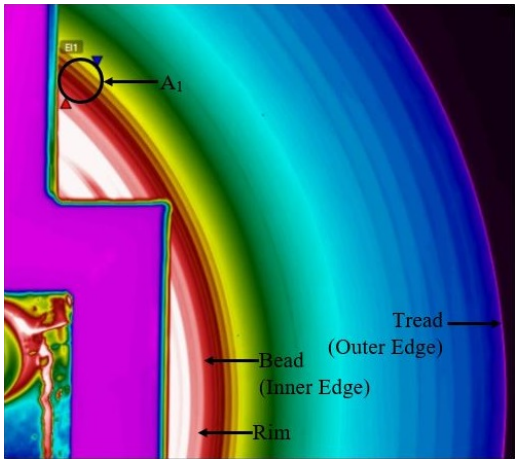

Figure 3 - Thermal Image of Tyre Inner Sidewall

Figure 3 shows a thermal image of the single, aluminium-rimmed wheel for $P_b = 4\ kW$. From these images the radial temperature distribution can be plotted versus time as shown in Figure 4 where 0% *radial position* denotes the inner edge of the bead and 100% *radial position* denotes the outer edge of the tread.

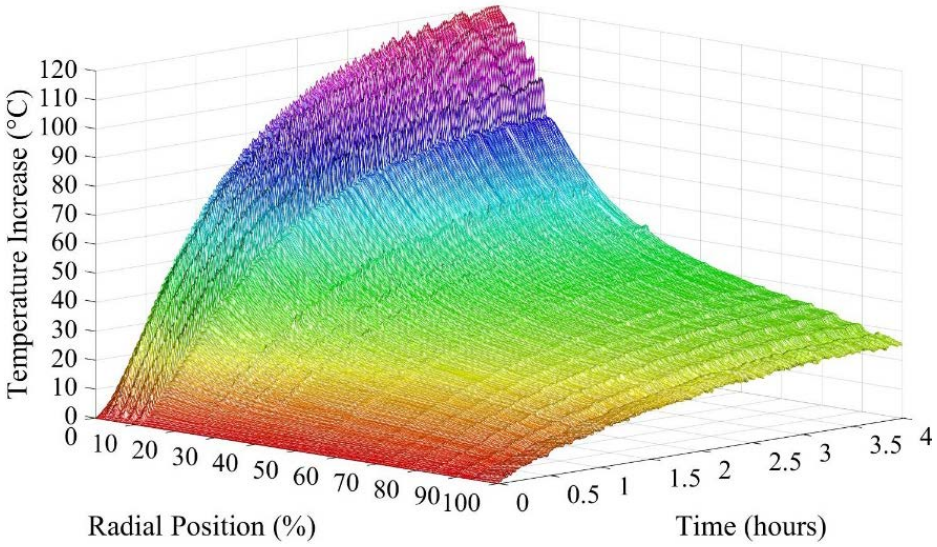

Figure 4 - Radial Tyre Temperature Distribution (Single, Aluminium, $P_b = 4\ kW$)

Tyre temperature is seen to decrease exponentially with increasing radial position. Of interest is the maximum tyre temperature since it will cause the most degradation of the rubber. The average temperature in the region A_1 in Figure 3 is thus isolated for investigation as the maximum tyre temperature.

Results are presented in terms of temperature increase from the onset of braking to offset differences in initial conditions. The average initial brake and maximum tyre temperatures were 30 ℃ and 32 ℃ respectively with ambient temperatures of approximately 25 ℃.

4. Results and Discussion

4.1 Maximum Tyre Temperature

The maximum tyre temperatures recorded for each wheel are plotted versus time in Figure 5 to Figure 8. Tyre temperature rose by between approximately 12 ℃ and 100 ℃ depending on wheel configuration and braking power. In general, the tyre temperatures of the aluminium-rimmed wheels were higher than those of the steel-rimmed wheels and the single wheel tyres were hotter than the duals. Temperature also increases with increasing braking power.

Variations in test conditions impact on the temperature response recorded during a test. Such factors include ambient temperature, humidity and ventilative airflow though the facility. The average of the four curves (plotted with the experimental data and labelled 'Mean') represents the tyre's temperature response to the mean of the braking powers - approximately 2.5 kW. This increases the overall accuracy of the experiments.

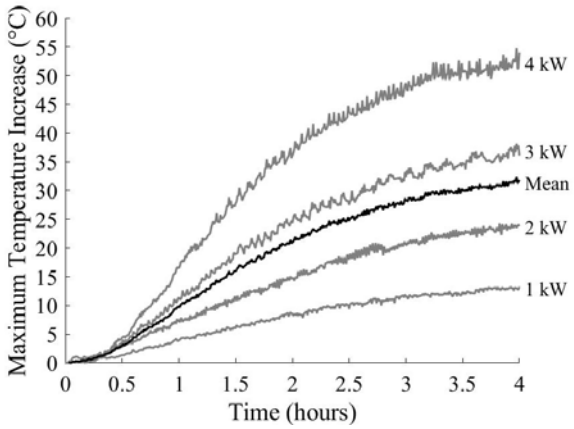

Figure 5 – Maximum Tyre Temperature Increase (Dual, Steel)

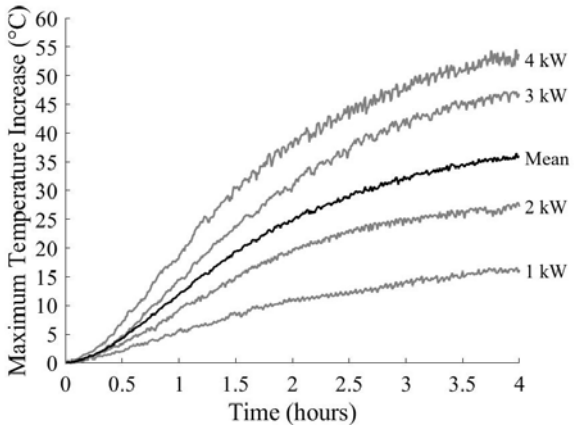

Figure 6 - Maximum Tyre Temperature Increase (Dual, Aluminium)

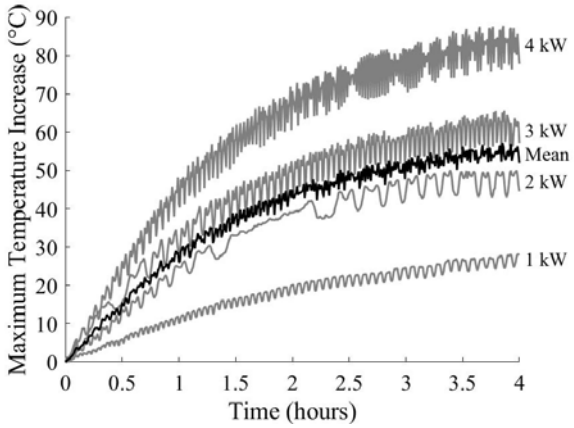

Figure 7 - Maximum Tyre Temperature Increase (Single, Steel)

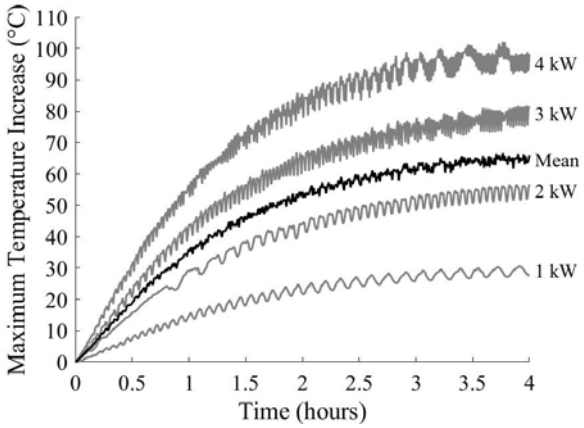

Figure 8 - Maximum Tyre Temperature Increase (Single, Aluminium)

The averaged response of each wheel was normalised by dividing the temperature values by the mean braking power. The resulting curves are plotted in Figure 9. The normalised curves behave as overdamped, second-order systems where the temperature output, $T(t)$ [℃], varies

as a function of time, $t\ [s]$, in response to a step input in braking power, $P_b\ [W]$. For initial conditions $T(t) = 0, \dot{T}(0) = 0$, such a system can be modelled using Equation 1.

$$T(t) = \frac{P_b}{k}\left(\frac{S_2}{S_1 - S_2}e^{S_1 t} - \frac{S_1}{S_1 - S_2}e^{S_2 t} + 1\right) \quad (1)$$

Where $S_1 = -1/\tau_1, S_2 = -1/\tau_2$. τ_1 and τ_2 have units $[s]$ and are known as the time constants of the system. These values determine the rate at which transient effects decay. The *stiffness* of the system, $k\ [W/°C]$, relates the magnitudes of $T(t)$ and P_b. MATLAB was used to fit Equation 1 to each set of averaged and normalised data; giving the model parameters listed in Table 3. Fitted curves were generated and are plotted in Figure 9.

Assuming a unit input $(1\ kW)$ the value $1/k$ gives the steady-state temperature increase. The steady-state maximum tyre temperatures of the aluminium rims were calculated to be 13% and 16% higher than those of the steel rims for the dual and single wheels respectively. This is attributed to increased conductive heat transfer from the brakes, through the rims and into the tyre. From the one-dimensional, steady-state form of Fourier's law, the rate of conductive heat transfer is directly proportional to thermal conductivity and inversely proportional to the length of the conductive path. Comparing the ratio of thermal conductivity to rim thickness for the two rims suggests that the aluminium rims will transmit heat approximately $85\% - 90\%$ more effectively than steel rims. This estimation is based on a simplified model which provides insight into why the tyres on the aluminium rims are hotter than those on the steel rims.

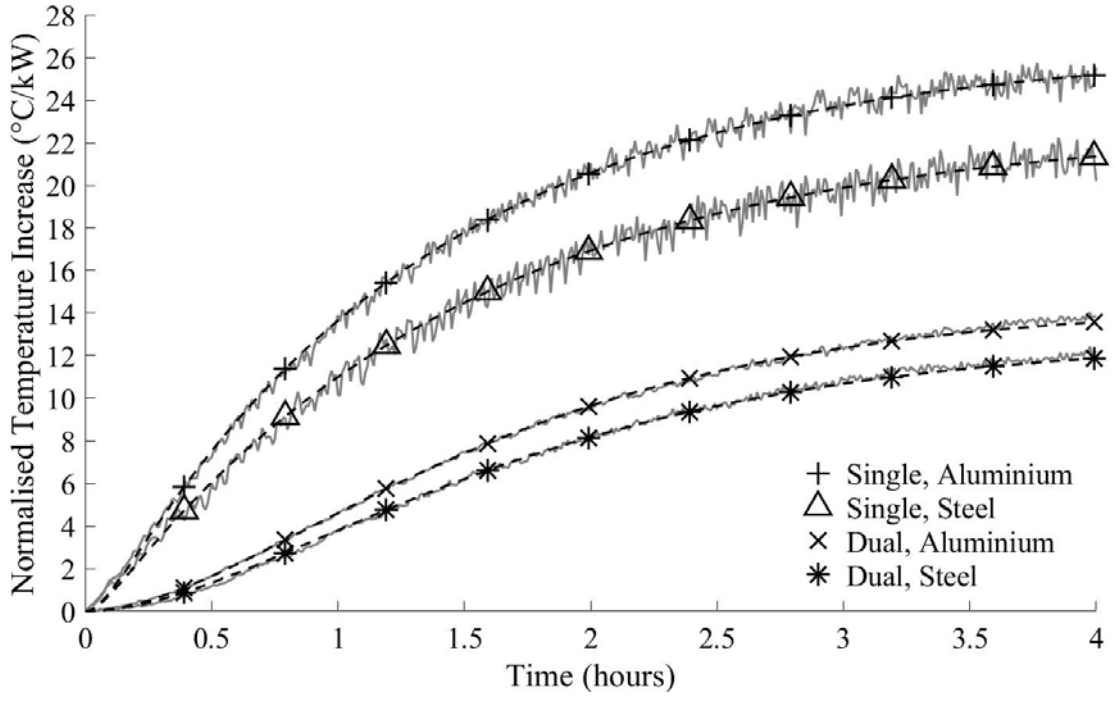

Figure 9 – Comparison of Maximum Tyre Temperature Responses Normalised per Kilowatt Braking Power

Wheel configuration has the largest impact on tyre temperature. The maximum tyre temperature change of the single wheels are 79% and 84% higher than those of the dual wheels for steel and aluminium rims respectively. This is attributed to the increased convective surface areas of the dual wheel configurations and the location of the tyre temperature measurements. The dual

wheel tyres have two additional sidewalls and a total surface area more than 80% higher than the single wheel tyres. This enhances convective cooling and thereby lowers their steady-state tyre temperature. The surface areas of the dual rims are also greater than those of the single rims however this is difficult to quantify for such irregular geometry.

Table 3 - Maximum Tyre Temperature Response Model Parameters

Parameter	Wheel Configuration			
	Dual, Steel	Dual, Aluminium	Single, Steel	Single, Aluminium
$\tau_1[s]$	3297	3120	5140	4582
$\tau_2\ [s]$	3297	3120	211.9	257.6
$K\ [W/℃]$	78.5	69.6	43.9	37.9
$RMSE$ [℃]	0.4	0.1	1.3	1.0
$Adjusted\ R^2$	0.9985	1.0000	0.9932	0.9972

For the dual wheels, the side by side or centre sidewalls will exhibit higher temperature changes than the inner sidewall owing to their proximity to the brake. Spatial restrictions make it impractical to measure the temperature at this location while the wheel is in motion. The maximum tyre temperatures stated for the dual wheels are underestimated, and the differences between maximum tyre temperatures for the two configurations are therefore less pronounced than reported in this study.

Comparing the stiffness values, the (steady state) the inner tyre sidewall temperature of a single, aluminium-rimmed wheel will increase up to 107% more than that of a dual, steel-rimmed wheel. For the 4 kW braking tests, the maximum inner sidewall temperatures of the dual, steel-rimmed wheel and single, aluminium-rimmed wheel reached 84 ℃ and 130 ℃ respectively over the four-hour test interval.

4.2 Brake Shoe Temperature

The brake shoe temperatures recorded for all four wheels are plotted versus time in Figure 10. The difference in brake temperature between the configurations is neither pronounced nor consistent. The changes in comparative temperature increase of the wheels across braking powers are insignificant and can be attributed to experimental error.

As with tyre temperature, the brake shoe temperatures were averaged and normalised. The parameters listed in Table 4 were obtained by fitting Equation 1 to the normalised curves using MATLAB. Comparing the stiffness values shows no difference in steady state temperature between the dual and single wheel brake shoes. This suggests that the geometry of the wheel does not affect brake cooling.

Table 4 - Brake Shoe Temperature Response Model Parameters

Parameter	Wheel Configuration			
	Dual, Steel	Dual, Aluminium	Single, Steel	Single, Aluminium
$\tau_1[s]$	3386	3095	3059	3039
$\tau_2\ [s]$	226.3	237.9	254.1	260.5
$K\ [W/℃]$	16.4	17.0	16.4	17.0
$RMSE$ [℃]	1.1	1.0	1.2	1.2
$Adjusted\ R^2$	0.9994	0.9994	0.9992	0.9992

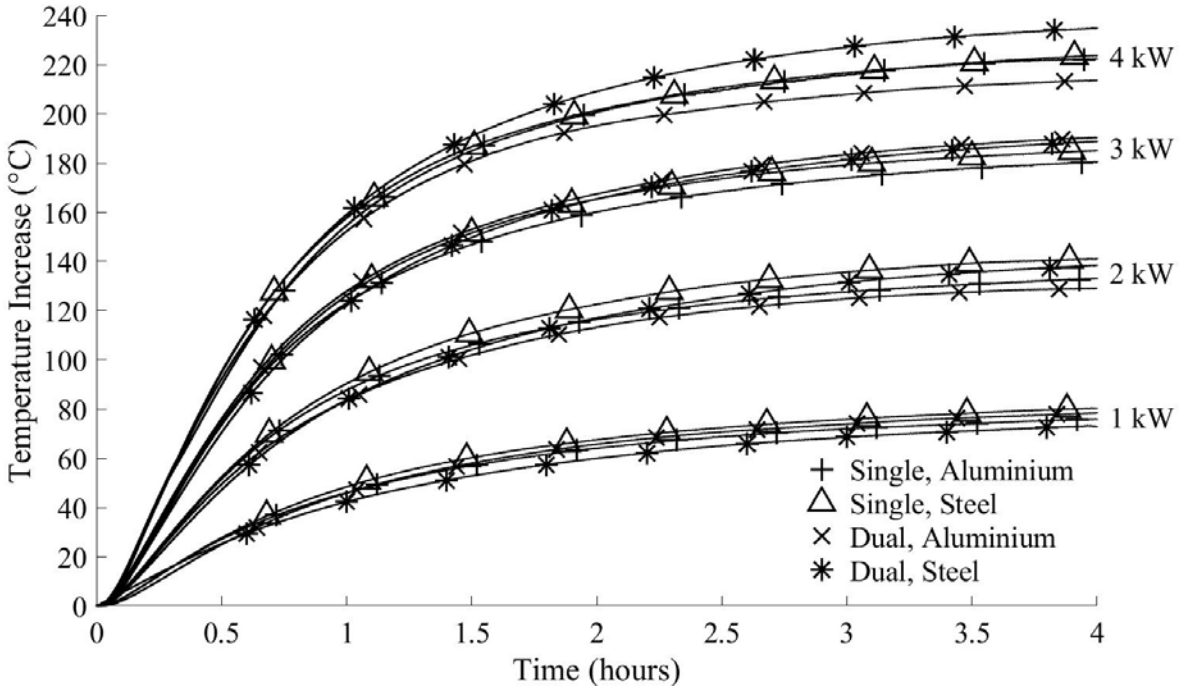

Figure 10 – Comparison of Brake Shoe Temperature Responses ($\mathbf{1\ kW \leq P_b \leq 4\ kW}$)

The brake shoe does run hotter when using a steel rim, but only by 4% for both the dual and single wheels. This is due to the higher conductance of the aluminium rims which facilitate greater dissipation of the braking heat. The difference is however marginal which suggests that the primary mechanisms of brake cooling are convection and radiation which are not affected by rim material. The results of this study suggest that the advantages of aluminium in place of steel rims with respect to reduced brake temperature are not great enough to offset the accelerated tyre wear and risk of blowout.

4.3 Modelling of Brake Shoe and Maximum Tyre Temperature

The model parameters obtained for the averaged, normalised curves were used to calculate the maximum tyre temperatures and brake shoe temperatures for each wheel under $1\ kW - 4\ kW$ continuous braking. These results were evaluated against the experimental data to determine the validity of the second-order models. Figure 11 and Figure 12 illustrate how the single, aluminium-rimmed wheel's model compared to measured data.

The metrics used to evaluate the models are the root-mean-square error ($RMSE$) and the percentage error which is calculated by dividing the $RMSE$ by the steady-state temperature of the curve in question. Table 5 lists the evaluation metrics for the maximum tyre temperature models. The models show a maximum percentage error of 10% which corresponds to an $RMSE$ of 2.4 ℃. The maximum $RMSE$ was 4.2 ℃ giving an error of 4%. Equation 1 is therefore valid for modelling maximum tyre temperatures up to approximately 170 ℃.

The evaluation metrics for the brake shoe temperature models are listed in Table 6. For $P_b = 1\ kW$ and $P_b = 4\ kW$ the brake shoe temperature models disagree severely with experimental data. Equation 1 assumes a linear system which is valid when conduction and convection are the only relevant heat transfer mechanisms. This model cannot correctly account for radiation since it is a function of the difference of temperatures to the fourth power and is thus a highly nonlinear phenomenon.

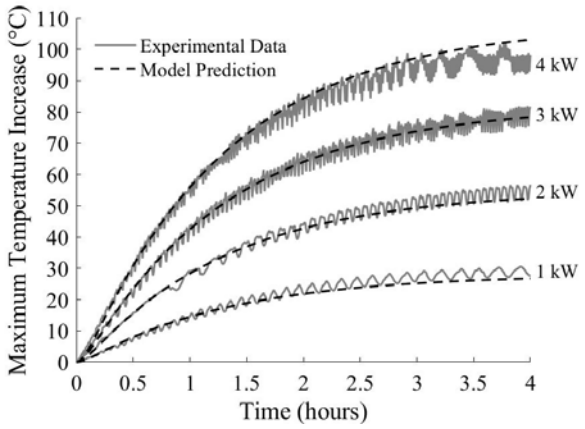

Figure 11 - Maximum Tyre Temperature Model Evaluation (Single, Aluminium)

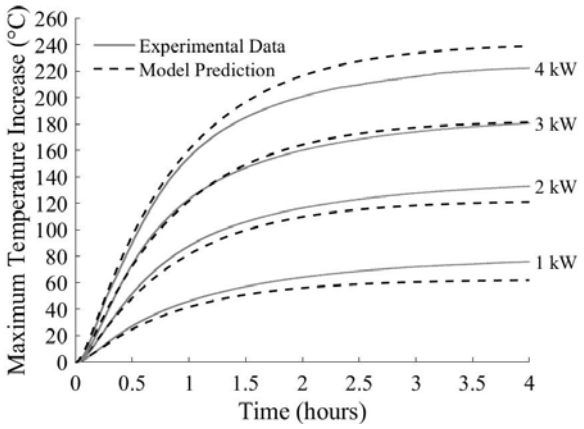

Figure 12 - Brake Shoe Temperature Model Evaluation (Single, Aluminium)

Table 5 - Maximum Tyre Temperature Modelling Evaluation

P_b $[kW]$	Wheel Configuration							
	Dual, Steel		Dual, Aluminium		Single, Steel		Single, Aluminium	
	$RMSE$ [°C]	$Error$ [%]	$RMSE$ [°C]	$Error$ [%]	$RMSE$ [°C]	$Error$ [%]	$RMSE$ [°C]	$Error$ [%]
1	0.3	2	0.7	4	2.4	10	1.8	6
2	1.6	6	0.9	3	3.7	8	2.0	4
3	0.9	2	2.4	5	4.0	6	2.3	3
4	3.0	6	1.8	3	4.2	4	3.7	3
$Average$	1.5	4	1.5	4	3.6	7	2.5	4

At higher temperatures, radiation is non-negligible and enhances the cooling of the brake shoe. At low temperatures, radiative heat transfer will be practically zero. The curve fitting procedure averages out the effects of radiation; causing the model to underpredict brake shoe temperatures for lower braking powers and overpredict for high braking powers. Nonlinear effects must be included in future work if the brake shoe temperature response is to be accurately modelled. Since the inaccuracy is common to all four wheels, the comparative evaluation of brake shoe temperature is still valid.

Table 6 - Brake Shoe Temperature Modelling Evaluation

P_b $[kW]$	Wheel Configuration							
	Dual, Steel		Dual, Aluminium		Single, Steel		Single, Aluminium	
	$RMSE$ [°C]	$Error$ [%]	$RMSE$ [°C]	$Error$ [%]	$RMSE$ [°C]	$Error$ [%]	$RMSE$ [°C]	$Error$ [%]
1	4.8	7	9.5	15	11.0	17	8.8	14
2	6.3	5	4.4	4	11.0	9	7.6	6
3	1.5	1	5.7	3	2.4	1	2.8	2
4	10.3	4	18.7	8	20.0	8	13.6	6
$Average$	5.7	4	9.6	8	11.1	9	8.2	7

In practice, such low braking powers are unlikely as are such elongated cycles. These models can however be used to estimate the maximum tyre temperature of different wheel configurations during more realistic alpine driving conditions.

South African regulations permit a heavy vehicle to travel at $40\ km/h$ on gradients up to 9%. For a 7-axle truck with a gross mass of 50 metric tonnes each wheel will dissipate $17.45\ kW$ of braking power to maintain a constant downhill speed. This assumes that 50% of the required braking power is achieved by rolling resistance, drag, and other auxiliary retarding effects.

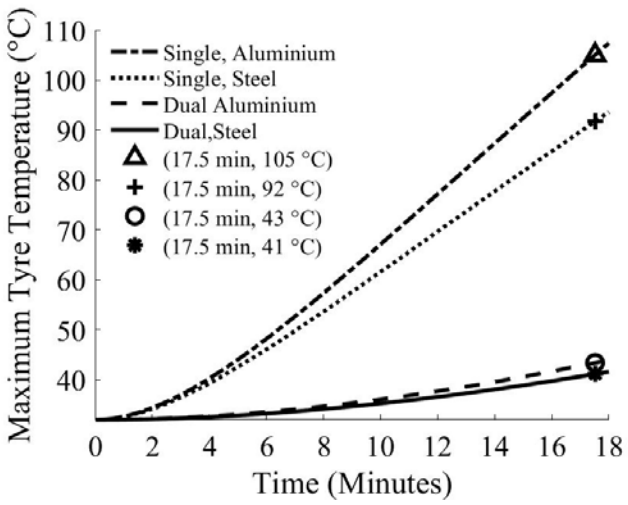

Figure 13 - Maximum Tyre Temperature Model for $P_b = 17.45\ kW$

Using the model parameters listed in Table 3 and an initial maximum tyre temperature of 32 ℃, the maximum tyre temperature response of each wheel was calculated and plotted in Figure 13. Tyre degradation will begin between 90 ℃ and 120 ℃. The maximum tyre temperature of the single, aluminium-rimmed wheel has reached the midpoint of this range after approximately 17 minutes. At the same time, the single, steel-rimmed wheel's tyre is cooler, although it has still been raised beyond safe temperature limits. The temperatures of the dual wheels are nearly identical – both being well below 90 ℃. This shows that, for more realistic braking conditions, single wheels will experience drastically increased tyre wear and have a far higher risk of blowout. This problem is exacerbated further by aluminium rims.

For the above scenario, the temperature responses are transient and are dominated by the thermal capacities of the rims. The higher the thermal capacity of the wheel, the more heat must be absorbed before it reaches a temperature where the rate of convection to the air is equal to the rate of conduction from the brake. The dual steel rims, for example, have an additional $11.5\ kg$ of steel and $62.5\ kg$ of tyre rubber. This increases the thermal capacity of the dual wheel by 77% over that of the single. For a given rim material, the dual wheels will exhibit a slower temperature rise than a less massive wheel subject to the same heating rate.

5. Conclusions

- For alpine braking, the reduced convective surface area of single wheels increases maximum tyre temperature beyond safe limits leading to accelerated wear and a heightened risk of blowout.
- The increased thermal conductance of aluminium rims facilitate enhanced conduction of braking heat into the tyre. This increases the maximum tyre temperature, exacerbates wear and increases the risk of blowouts.
- The reduced thermal capacity of the single wheels decreases the maximum allowable braking time before the tyres reach unsafe temperatures.
- Wheel configuration and rim material have no significant effect on brake temperature.

- Maximum tyre temperature can be accurately modelled using a linear, lumped-mass system equation for temperatures up to 170 ℃.
- Linear, lumped-mass models will overpredict brake shoe temperatures for higher braking powers and underpredict brake shoe temperatures for lower braking powers owing to the nonlinear behaviour of radiative cooling.

6. Future Work

Future work will focus on deriving lumped-mass brake and tyre models using energy balances. This will yield equations which explicitly relate component temperature to braking power in terms of bulk physical parameters such as mass, conductivity and specific heat. For brake shoe temperatures, radiative effects will be included.

Better understanding of the relationship between vehicle speed and convective cooling will broaden the validity of the models. Further experimentation will be conducted to quantify the impact of changing velocity on the temperature responses. The maximum temperatures of the side by side sidewalls of the dual wheels will be measured and compared to the maximum temperatures of single wheels' inner sidewalls.

Having obtained the time constants for a system it is possible to model the temperature response to any braking profile. Further work is being done on predicting tyre temperature for urban driving conditions. Figure 14 was generated to illustrate the maximum tyre temperature response of a truck during a simplified stop-start driving cycle. Each wheel of the vehicle is assumed to dissipate $20\,kW$ of braking power for 10 seconds every 5 minutes.

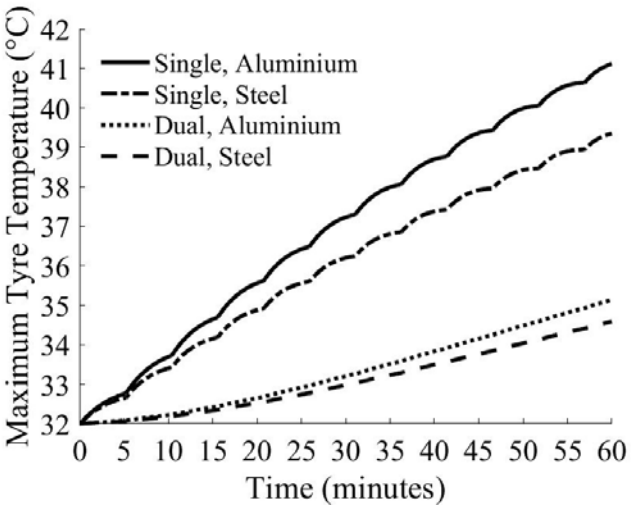

Figure 14 - Maximum Tyre Temperature Model for $20\,kW$ Repeated Braking

A series of repeated braking cycles will be simulated in SIMULINK and validated by laboratory tests. Time-varying power inputs for realistic, urban driving conditions will be determined and used to simulate the maximum tyre temperatures on an actual heavy vehicle. This is beneficial to understanding the thermal wear of tyres for new rim designs and wheel configurations.

7. Acknowledgements

The authors would like to thank Siemens Southern Africa for donating the motor and gearbox for the custom-built test rig; BPW South Africa for the single and dual axles and aluminium rims; CA Muller for the steel dual rims; CT Hydraulics, Fluid Power Group, Hydraulic Training and Consultants and Ax. Hydraulics for the hydraulic system, and SKF South Africa for the bearings.

References

- Benoit, R. *et al.* (2009), Heavy Vehicles Tire Blowout and Explosion, Montréal.
- Day, A. (2014), Braking of Road Vehicles, Oxford: Elsevier.
- Hart, P. M. (2012), "A review of truck fire causation", in Proc. 12th Int. Symposium on Heavy Vehicle Transportation Technology, Stockholm.
- Luo, R. K., Mortel, W. J. and Wu, X. P. (2015), "Investigation on rubber failure due to heat generation under dynamic loading", Proc. IMechE, Part L: Journal of Materials: Design and Applications, 229(1), pp. 77–87.
- Malzahn, Y. and Kienhöfer, F. (2014), "The effect of wheel configuration on vehicle component temperatures", in Proc. 13th International Symposium on Heavy Vehicle Transport Technology", San Luis.
- Road Traffic Management Corporation (2016), "RTMC commends Mpumalanga for impounding un-roadworthy trucks", Press Release, 6 July. Available at: http://www.rtmc.co.za/rtmc1/Docs/Mpumalanga impounding.pdf.
- Road Traffic Management Corporation (2017), "Truck accidents claim 24 lives and 69 injuries in 24-hour period", Press Release, 4 July. Available at: http://www.rtmc.co.za/images/documents/24 die in two trucks accidents.pdf.
- Sokolov, S. L. (2009), "Analysis of the heat state of pneumatic tires by the finite element method", Journal of Machinery Manufacture and Reliability, 38(3), pp. 310–314.
- Welty, J. R., Rorrer, G. L. and Foster, D. G. (2015), Fundamentals of Momentum, Heat and Mass Transfer, Sixth, Singapore: John Wiley & Sons.
- Zhao, Y. *et al.* (2008), "Frictional Wear and Thermal Fatigue Behaviours of Biomimetic Coupling Materials for Brake Drums", Journal of Bionic Engineering, 5(SUPPL.), pp. 20–27.